

• Supplementary File •

Continuous-wave 2.9-3.8 μm random lasing via temperature-tuning free difference-frequency generation of random fiber lasers in PPLN crystal

Bo HU¹, Han WU^{1*}, Kan TIAN¹ & Houkun LIANG^{1*}

¹College of Electronics and Information Engineering, Chengdu, Sichuan, 610064, China

Appendix A Experimental setup

The dash box of Fig. A1 presents the configuration of the tunable YRFL (DFG pump source) which consists of the tunable YRFL seed and the power amplifier. A 976 nm laser diode (LD) is used as pump for the YRFL seed, which is injected into a 5 m-long ytterbium-doped fiber (YDF, Nufern LMA-YDF-10/130) through a $(2+1) \times 1$ combiner. A 1:1 coupler-based fiber loop mirror is connected to the signal port of the combiner and a wavelength tunable filter (WL Photonics Inc., WLTF-NM) with 0.1 nm -3 dB bandwidth is integrated into the fiber loop mirror to provide the wavelength-selectable point feedback. Although the used filter is manual tunable one in our experiment, electric tunable filter is also commercially available with the tuning speed up to 80 nm/sec, which can fulfil the fast wavelength tuning requirement of DFG source compared to the conventional temperature tuning. By means of active gain in the YDF, the wavelength-selectable point reflection and the distributed random Rayleigh feedback in a 5 km-long single-mode fiber (SMF), the ytterbium-doped random fiber lasing with tunable wavelength can be generated. The output power of YRFL is 300 mW with 3 W LD pump. Subsequently, the YRFL seed is further boosted in the power amplifier stage consisting of a 6 m-long YDF (Nufern LMA-YDF-10/130) and another LD pump. The output power of the tunable YRFL in the wavelength range of 1040 nm–1090 nm can be boosted to more than 8 W after the amplifier stage.

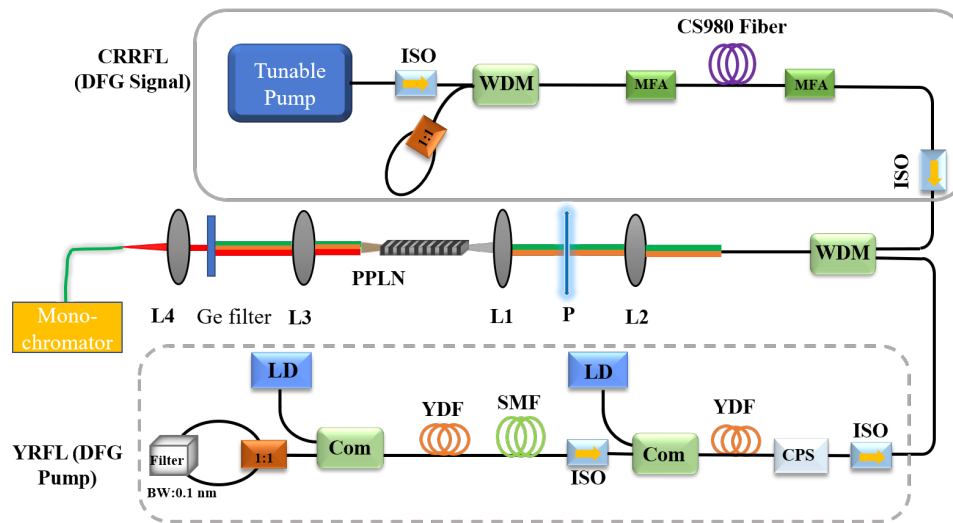


Figure A1 The schematic of experimental setup of the temperature-tuning free CW DFG of dual wavelength-tunable random fiber lasers in PPLN crystal. WDM, wavelength division multiplexer; MFA, mode-field adapter; ISO, isolator; CPS, cladding power stripper; LD, laser diode; YDF, ytterbium-doped fiber; SMF, single mode fiber; Com, pump combiner; L, lens; P, polarizer. Ge, Germanium filter.

The solid box of Fig. A1 depicts the configuration of tunable CRRFL (DFG signal source). To generate the wavelength-tunable cascaded random Raman lasing, a tunable ytterbium-doped fiber laser [1] is used as the pump source for CRRFL. To realize the CRRFL beyond 1.8 μm , a section of 3.5 km-long Raman fiber (CS980/125-20/250, YOFC) which has a zero-dispersion-wavelength longer than 1.8 μm [2] is used to provide Raman gain and random distributed feedback for cascaded random Raman lasing. The tunable pump is connected to an isolator (≤ 1 dB insertion loss and ≥ 30 dB isolation in the range of 1040-1090 nm) and then injected into the Raman fiber via the Pass port of a wavelength division multiplexer (WDM, Pass port: 1040-1090 nm, Reflection port: 1100-1700 nm). Meanwhile, a 1:1 coupler-based fiber loop mirror is connected to the Reflection port of WDM to provide broadband point feedback for each order of random Raman lasing. The pigtail fiber of WDM has a core diameter about 10 μm ,

* Corresponding author (email: hanwu@scu.edu.cn, hkliang@scu.edu.cn)

while the CS980 fiber has a core diameter about 4 μm . Therefore, we insert a 10/4 μm mode-field adaptors (MFA) between WDM and CS980 fiber to reduce the splicing loss. A wideband isolator (1.2 dB insertion loss @1500 nm and 1 dB insertion loss @1630 nm, isolation ≥ 20 dB in the range of 1500-1650 nm) with the operating wavelength range around 1.58 μm is connected at the output of CRRFL to minimize the backward reflection.

The DFG is carried out by using a PPLN crystal in a single-pass configuration. The tunable YRFL and CRRFL are combined by another WDM (Pass port: 1040-1090 nm, Reflection port: 1100-1700 nm) and collimated with a broadband fiber collimator. Since both the YRFL and CRRFL are depolarized sources, the collimated beam is made linearly polarized by a polarizer. The polarizer has antireflection coating in the wavelength range of 1-1.7 μm , we have measured the powers after PBS are about 50% and 46% of the total powers of YRFL and CRRFL, respectively. The polarized beam is then focused with a lens of 75 mm focal length into the PPLN crystal (HC Photonics) with the antireflection coatings at pump, signal and idler wavelengths. The dimensions of the PPLN crystal are 1 (height) \times 1 (width) \times 25 (length) mm^3 . Two separate poled gratings with the periods of 30.10 and 31.15 μm are used in the experiment with the crystal temperature fixed at 40 $^\circ\text{C}$. The estimated beam diameters at focus are 45.4-47.3 μm and 65-71.3 μm for the pump laser (in the range of 1045-1090 nm) and signal laser (in the range of 1495-1643 nm), respectively. Meanwhile, the Rayleigh lengths inside the crystal are estimated to be about 3.43-3.55 mm and 4.9-5.35 mm for the pump and signal laser, respectively. And the generated DFG signal from the crystal is collimated by a CaF_2 lens with 50 mm focal length. An antireflection-coated Germanium filter is used to block the residual pump and signal beams, and the output power of the generated DFG is measured by a power meter (Ophir, 3A). For spectral measurement, the DFG radiation is coupled into a hollow core MIR fiber (OptoKnowledge HF500MW) with a 500 μm core diameter focused by another CaF_2 lens with a 50 mm focal length, and a grating-scanning monochromator (Zolix Omni-500i) with a liquid nitrogen cooled HgCdTe detector (Judson, DMCT16-De01) is then used to record the spectrum of MIR radiation.

Appendix B Output characteristics of YRFL and CRRFL

Appendix B.1 Output characteristics of YRFL

The output characteristics of the proposed DFG pump, i.e., tunable YRFL are shown in Fig. B1. The spectra and output power of YRFL are measured after polarizer. The power of the LD pump in the amplifier stage is set as 16 W. The wavelength of YRFL could be continuously tuned from 1045 nm to 1090 nm, and the -3 dB bandwidths of the YRFL are approximately 0.2 nm in the entire tuning range. Meanwhile, it can be seen that the ASE is more significant when the central wavelength of YRFL is in the range of 1045-1055 nm. However, the random lasing still has very high signal to noise ratio (the signal peak power to ASE peak power) and the power ratio of the integral ASE intensity is 4.19% for 1045 nm YRFL and is only 0.7% for 1055 nm YRFL. The output powers after polarizer as a function of the tuning wavelengths are plotted in Fig. B1(b). It is observed that the output powers of different lasing wavelengths are in the range of 4.15-4.6 W with a fluctuation less than 9.3%. It is worth mentioning that the output power of YRFL could be further increased by using more powerful LD source in the amplifier stage.

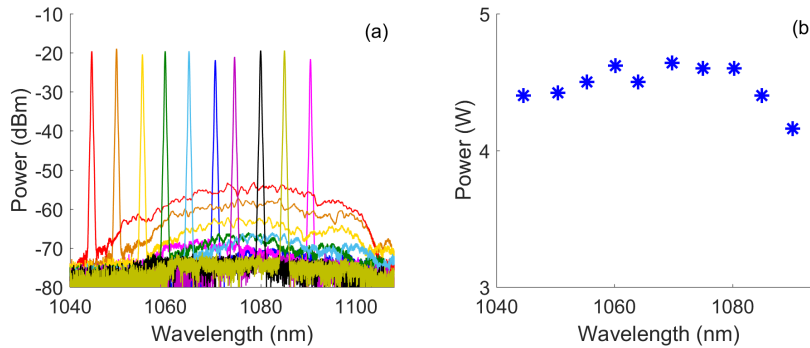


Figure B1 (Color online) Output characteristics of tunable YRFL. (a) normalized output spectra of tunable YRFL. (b) output power after polarizer as a function of the YRFL's wavelength.

Appendix B.2 Output characteristics of CRRFL

The output characteristics of the 5th-order random Raman lasing of CRRFL are shown in Fig. B2(a) and Fig. B2(b). With the tunable pump in the range of 1065-1090 nm, the central wavelength of the 5th-order random Raman lasing can be continuously tuned from 1495 nm to 1535 nm. The -3 dB bandwidths are in the range of 2.5-4 nm. The output powers of the 5th-order random Raman lasing with different central wavelengths are measured after a polarizer, as shown in Fig. B2(b). The output power gradually increases from 0.58 W to 0.92 W at 11.5 W of pump power when the wavelength tunes from 1495 nm to 1535 nm due to the decrease of the loss coefficient of the Raman fiber used. The loss coefficient is measured as 1.8 dB/km and 1 dB/km at 1495 nm and 1535 nm, respectively. Similarly, the output properties of the 6th-order random Raman lasing of CRRFL are depicted in Fig. B2(c) and Fig. B2(d) when the pump power is increased to 15 W. The wavelength tuning range is 1595 to 1642 nm with output powers of 1.02-1.2 W. The -3 dB bandwidths of different central wavelengths are measured in the range of 3-4.5 nm. The spectra of CRRFL exhibit double peak structure which corresponds to the two Raman gain maxima of the silica fiber, and the calculated power ratio of the dominated peak is at least 65%. The length of fiber has a significant effect on the threshold, efficiency and maximum output power of random fiber lasers. In our experiment, we have tested by using longer fiber length, the threshold of random lasing would not change. However, the output power of CRRFL decreases due to the additional loss induced by the longer fiber length. By decreasing the fiber length, the measured results show significant increase of the lasing threshold for CRRFL. Due to the limited pump power, we optimize the CS980 fiber length as 3.5 km and we note that the output power of CRRFL could be further boosted by using more powerful pump together with shorter fiber length [3].

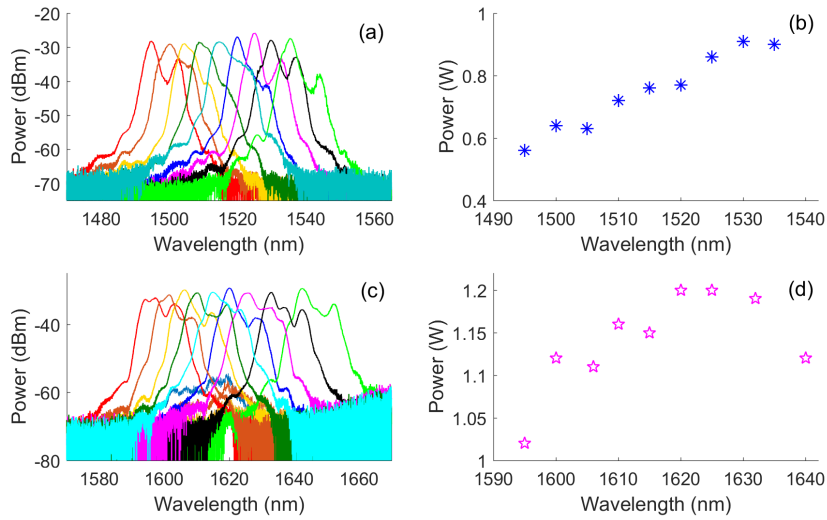


Figure B2 (Color online) Output characteristics of CRRFL. (a) normalized output spectra of the 5th-order random Raman lasing. (b) output power as a function of the wavelength when the pump power is 11.5 W. (c) normalized output spectra of the 6th order RFL. (d) output power as a function of the different 6th RFL wavelength when the pump power is 15 W.

Appendix B.3 Time-domain characteristics of YRFL and CRRFL

Since the YRFL and CRRFL are both of relatively broad linewidth, the used random fiber lasers feature the low temporal coherence with the fast temporal intensity fluctuations on the scale of ps. In order to measure the temporal dynamics of YRFL at 1055.3 nm and CRRFL at 1609.8 nm at maximum output power, we use the photodetector (Thorlabs DET08C/M) with 5 GHz bandwidth and the oscilloscope (RS RTO2024) with 2 GHz bandwidth. The optical bandwidth of YRFL and CRRFL are both much higher than the bandwidth of oscilloscope, and thus the fluctuation time is determined by the bandwidth of oscilloscope. We can clearly see the fast temporal intensity fluctuations for both the YRFL and the CRRFL, as shown in Fig. B3(a) and B3(c). We also calculate the time-to-time intensity fluctuations correlation map plotted in Fig. B3(b) and (d) for the YRFL and CRRFL, respectively. The results indicate that the intensity fluctuations within the measurement window are fully uncorrelated for both the YRFL and the CRRFL. Therefore, though DFG process, the generated MIR random lasing could also inherit the fast and random temporal intensity fluctuations, making it suitable for performing temporal ghost imaging [4, 5] and chaotic Lidar [6, 7].

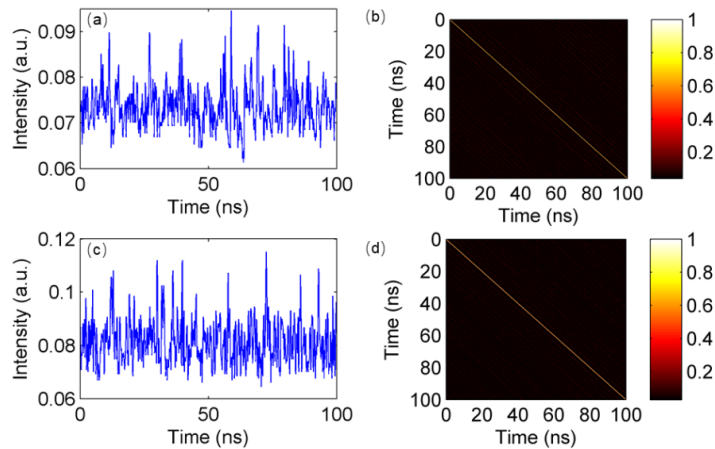


Figure B3 (Color online) (a) Temporal intensity fluctuations of YRFL over a 100 ns time window; (b) Time-to-time intensity fluctuations correlation map of YRFL calculated over 1000 temporal windows; (c) Temporal intensity fluctuations of CRRFL over a 100 ns time window; (d) Time-to-time intensity fluctuations correlation map of CRRFL calculated over 1000 temporal windows.

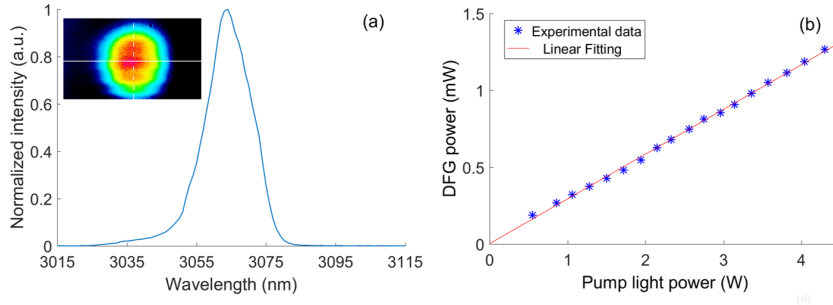


Figure C1 (Color online) Output characteristics of idler with 3064 nm of central wavelength. (a) normalized output spectrum, the upper inset shows the beam profile of idler radiation, measured by a MIR camera (Dataray, Win-CamD-FIR8-14-HR), which confirms near-Gaussian beam distribution of the MIR random lasing. (b) DFG power as a function of input power of pump source.

Appendix C Output characteristics of DFG

Appendix C.1 Experimental results of MIR laser centered at wavelength 3064 nm

Appendix C.2 Phase-matching condition description

As shown in Fig. C2(a), for the grating period of 30.10 μm period, by tuning the pump wavelength from 1045 to 1090 nm, phase-matching condition can be satisfied to generate idler radiation from 3.4 to 3.8 μm by simultaneously tuning the signal wavelength from 1500 nm to 1530 nm, which is within the tuning range of the 5th-order random Raman lasing of CRRFL. Similarly, the required signal wavelength tuning range is 1595-1635 nm to realize an idler emission from 2.9 to 3.4 μm in PPLN with 31.15 μm grating period (see in Fig. C2(b)), which can be satisfied by using the 6th-order random Raman lasing of CRRFL. Fig. C2(c) presents the experimentally measured spectra of the MIR DFG random laser, with the wavelength continuously tuning from 2.9 μm to 3.8 μm , by varying the wavelength pairs of YRFL and CRRFL together with shifting between two different grating periods.

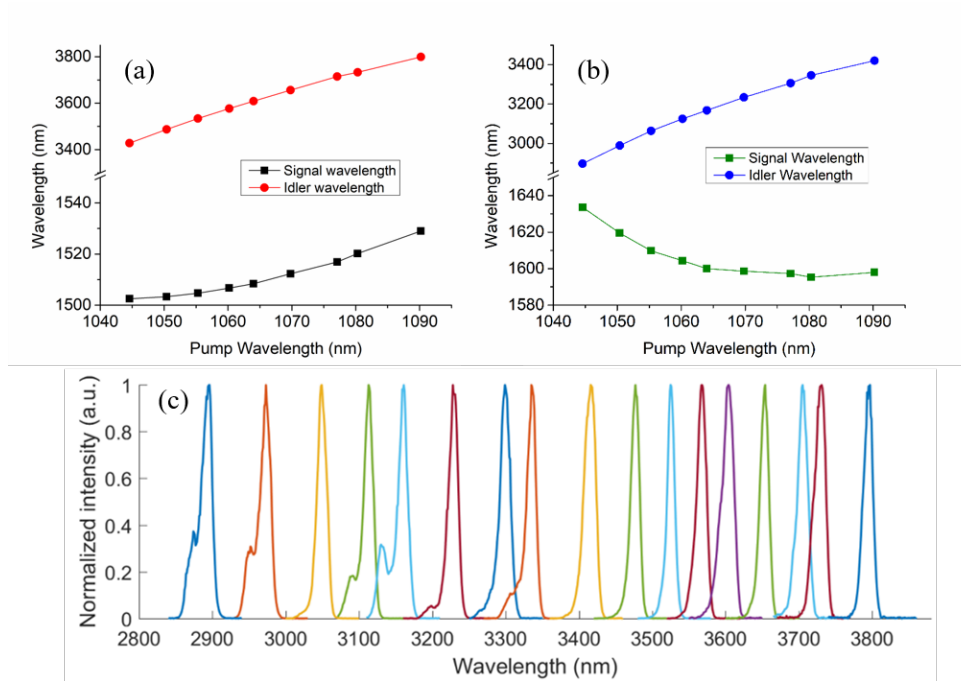


Figure C2 (Color online) Phase-matching conditions between signal, idler and pump wavelengths for (a) 30.10 μm of grating period and (b) 31.15 μm of grating period. (c) Experimental measured spectra of the tunable MIR random laser from 2.9 μm to 3.8 μm .

Appendix C.3 Output power of idler radiation as a function of idler wavelength

The output power of idler radiation as a function of idler wavelength is plotted in Fig. C3. More than 1 mW MIR output power is achieved for 2.9-3.3 μm idler wave. The idler power beyond 3.4 μm is lower due to the lower power of the 5th-order random Raman lasing than that of the 6th-order one, which can be clearly seen in Fig. B2(b) and Fig. B2(d).

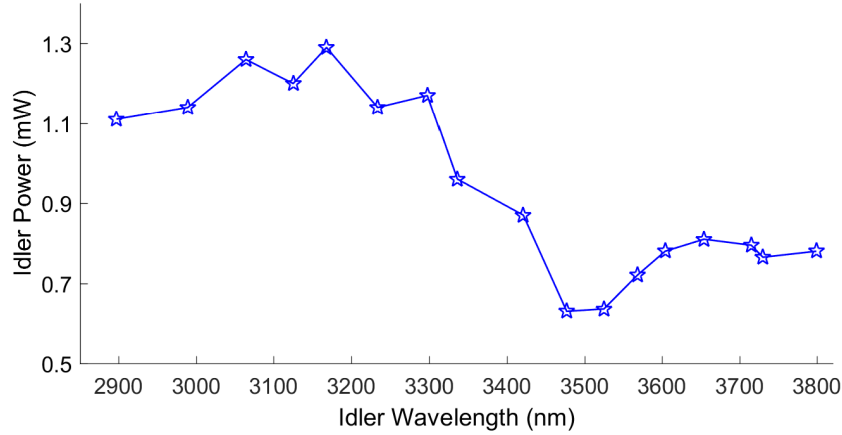


Figure C3 (Color online) Output idler power as a function of idler wavelength.

Appendix D Discussion results

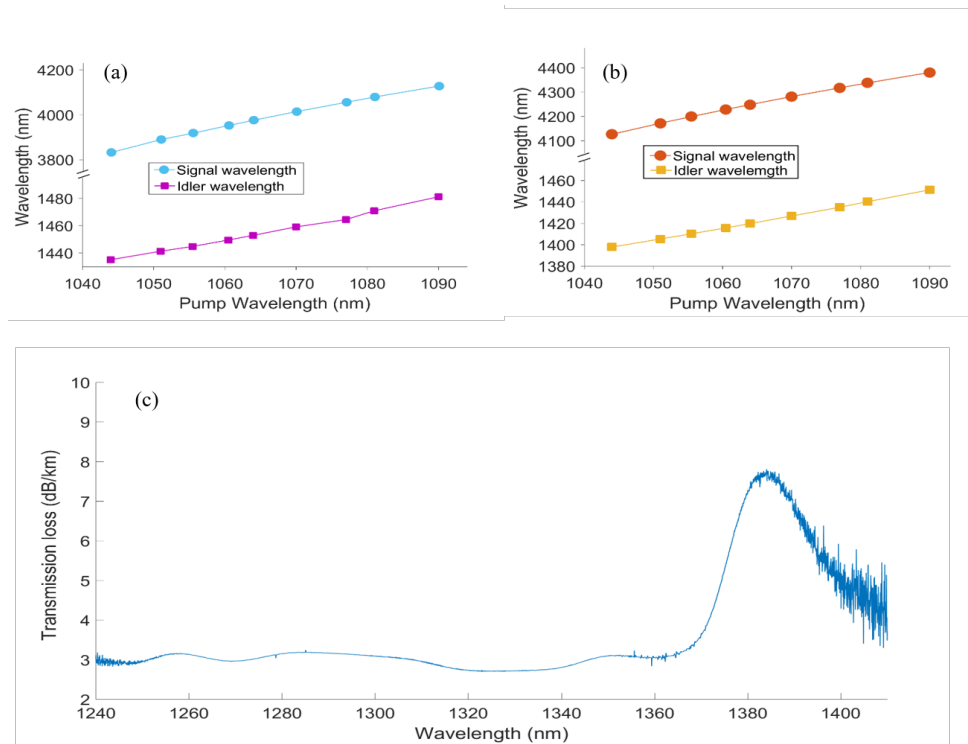


Figure D1 (Color online) Phase-matching conditions between signal, idler and pump wavelengths for (a) 29.13 μm of grating period and (b) 28.30 μm of grating period; (c) The experimentally measured transmission loss coefficient curve of the used Raman fiber in the range of 1260-1400 nm.

We calculate the phase-matching conditions in PPLN with grating periods of 29.13 and 28.30 μm , as shown in Fig. D1(a) and Fig. D1(b), respectively. The crystal temperature is still set as 40 $^{\circ}\text{C}$. It is confirmed that further extension of tuning range of DFG source to 4.4 μm can be realized by utilizing signal lasers in the range of 1430 nm-1480 nm and 1400-1450 nm. The DFG signal in these wavelength ranges can be provided by lower order random Raman lasing of CRRFL in principle. However, in our experiment, due to the existence of intense water absorption peak of the Raman fiber used, the generation of random lasing in 1370-1400 nm is prohibited, which further impedes the generation of cascaded random Raman lasing in 1460-1490 nm. Fig. D1(c) illustrates the experimentally measured transmission loss curve of the used Raman fiber (CS980/125-20/250, YOFC) by using a superluminescent light emitting diode (SLD) at a central wavelength of 1330 nm, and with a -30 dB bandwidth of 130 nm. The significant water absorption peak around 1385 nm with the loss coefficient up to 6.5 dB/km is clearly presented. However, this issue can be solved by using other type of Raman fiber with suppressed water absorption [8,9].

References

- 1 Han B, Rao Y, Wu H, et al. Low-noise high-order Raman fiber laser pumped by random lasing. *Opt. Lett.*, 2020, 45: 5804-5807.

- 2 Zhang Y, Song J X, Ye J, et al. Tunable random Raman fiber laser at 1.7 μm region with high spectral purity. *Opt. Express*, 2019, 27: 28800-28807.
- 3 Wang Z N, Wu H, Fan M Q, et al. High power random fiber laser with short cavity length: theoretical and experimental investigations. *IEEE J. Sel. Top. Quantum Electron*, 2015, 21: 0900506.
- 4 Wu H, Han B, Wang Z, et al. Temporal ghost imaging with random fiber lasers. *Opt. Express*, 2020, 28: 9957-9964.
- 5 Wu H, Ryzkowski P, Friberg A T, et al. Temporal ghost imaging using wavelength conversion and two-color detection. *Optica*, 2019, 6: 902-906.
- 6 Jumpertz L, Schires K, Carras M, et al. Chaotic light at mid-infrared wavelength. *Light: Sci. Appl*, 2016, 5: e16088.
- 7 Lin F Y, Liu J M, Chaotic lidar. *IEEE J. Sel. Top. Quantum Electron*, 2004, 10: 991-997.
- 8 Zhang L, Jiang H, Yang X, et al. Nearly-octave wavelength tuning of a continuous wave fiber laser. *Sci. Rep*, 2017, 7: 42611.
- 9 Dong J Y, Zhang L, Jiang H W, et al. High order cascaded Raman random fiber laser with high spectral purity. *Opt. Express*, 2018, 26: 5275-5280.